SANDIA REPORT

SAND2009-5333
Unlimited Release
Printed July 2009

Measurements of the Operating Characteristics of a 1064 nm Pumped KTP RISTRA OPO

Darrell J. Armstrong

Prepared by
Sandia National Laboratories
Albuquerque, New Mexico 87185 and Livermore, California 94550

Sandia is a multiprogram laboratory operated by Sandia Corporation,
a Lockheed Martin Company, for the United States Department of Energy's
National Nuclear Security Administration under Contract DE-AC04-94-AL85000.

Issued by Sandia National Laboratories, operated for the United States Department of Energy by Sandia Corporation.

Available to DOE and DOE contractors from
U.S. Department of Energy
Office of Scientific and Technical Information
P.O. Box 62
Oak Ridge, TN 37831

Telephone: (865) 576-8401
Facsimile: (865) 576-5728
E-Mail: reports@adonis.osti.gov
Online ordering: http://www.osti.gov/bridge

Available to the public from
U.S. Department of Commerce
National Technical Information Service
5285 Port Royal Rd
Springfield, VA 22161

Telephone: (800) 553-6847
Facsimile: (703) 605-6900
E-Mail: orders@ntis.fedworld.gov
Online ordering: http://www.ntis.gov/help/ordermethods.asp?loc=7-4-0#online

SAND2009-5333
Unlimited Release
Printed July 2009

Measurements of the Operating Characteristics of a 1064 nm Pumped KTP RISTRA OPO

Darrell Armstrong
Photonic Microsystem Technologies Department
Sandia National Laboratories
P.O. Box 5800
Albuquerque, NM 87185-1082
darmstr@sandia.gov

David Roberts, Jack Wood, Gary Gimmestad
Georgia Tech Research Institute
Electro Optics System Laboratory
925 Dalney Street
Atlanta, GA 30332
David.Roberts@gtri.gatech.edu

Abstract

Measurements of the operating characteristics of a 1064 nm pumped potassium titanyl phosphte (KTP) optical parametric oscillator (OPO) were carried out at the Electro Optics Systems Laboratory of Georgia Tech Research Institute (GTRI). The OPO was developed by Sandia National Laboratories and employs a nonplanar image-rotating geometry that is known by the acronym RISTRA, denoting Rotated Image Singly-Resonant Twisted RectAngle. The OPO was configured for pumping by the 1064 nm fundamental wavelength of a Q-switched Nd:YAG laser to generate a signal wavelength at 1627 nm and idler wavelength at 3074.8 nm. GTRI will be incorporate the OPO into a multi-wavelength lidar platform called the Integrated Atmospheric Characterization System (IACS). Prior to completion of the system design for the IACS platform, personnel at GTRI carried out a series of risk reduction experiments to measure the operating characteristics of the OPO. Sandia's role in this effort included technical assistance with numerical modeling of OPO performance, selection of nonlinear optical crystals, specification of cavity-mirror dielectric coatings, selection of vendors for optical components, and advice concerning integration of the RISTRA OPO into the IACS platform. This report

describes results of the risk reduction measurements and it also provides some background information on the operating characteristics of RISTRA OPO's but is not intended to be a tutorial. A working knowledge of pulsed solid-state lasers, laser cavity modes, laser beam quality and beam propagation, and three-wave mixing in nonlinear crystals, is useful.

Acknowledgment

This work was funded through a work for others contract, WFO proposal 017090108-0, with Georgia Tech Research Institute, Atlanta, GA.

Contents

Appendix

Figures

1 Introduction and background

The RISTRA OPO [1] provided by Sandia National Laboratories for the Integrated Atmospheric Characterization System was put through preliminary risk-reduction tests by personnel at the Electro Optics System Laboratory of Georgia Tech Research Institute (GTRI) during the weeks of 06/08/2009 and 06/22/2009. For GTRI's lidar application the OPO was configured for pumping by a Q-switched Nd:YAG laser at 1064 nm and contained two *xz*-cut potassium titanyl phosphate (KTP) crystals to generate a resonated signal wave at 1627 nm and a non-resonant idler wave at 3074.8 nm. To reduce the effects of parametric back conversion and thus enhance conversion efficiency, the cavity contained two crystals with unequal lengths of 14 mm, followed by 17 mm. The pump laser, a Continuum Inlite, and the OPO, were operated without injection seeding and therefore oscillated on multiple longitudinal modes. While the Inlite provides pulse energies > 475 mJ at 10 Hz in a compact, rugged package that is well suited for use in lidar platforms, we found its approximately 6.5 mm diameter semi-donut-shaped spatial fluence profile was less than optimum for pumping nanosecond OPO's. This was especially true for the RISTRA's non-planar image-rotating geometry because broadband oscillation in this cavity can support multiple non-degenerate off-axis Laguerre-Gaussian modes [2]. Given that the OPO's cavity Fresnel number was ~ 200,[1] pumping with a donut-shaped beam resulted in a signal beam spatial fluence profile that contained an admixture of these off-axis modes and exhibited lower than desired beam quality and a relatively high far field divergence angle of approximately 4 mrad.

Real world applications of crystal nonlinear optics often require accepting some degree of compromise, and in the case of GTRI's 1064 nm pumped KTP RISTRA OPO we accepted diminished beam quality to increase optical conversion efficiency. This was done by selecting mixing parameters where the pump and resonated signal waves share the same polarization, with $1064(o) \rightarrow 1627(o) + 3074.8(e)$ at $\theta = 72.9^\circ$ in the *xz*-plane.[2] This choice compensates for the smaller effective nonlinearity, d_{eff}, that would be obtained from another *xz*-cut of KTP at $\theta = 45.1^\circ$ where the polarizations of the mixing waves are more likely to achieve beam good quality with $1064(o) \rightarrow 1627(e) + 3074.8(o)$. The values of d_{eff} for these two *xz*-cuts of KTP are 3.32 pm/V and 2.29 pm/V, respectively, which have a small but significant difference because parametric gain for the OPO's signal field – in the absence of pump depletion – is exponential in the product gL where L is the crystal length, $g = [\Gamma^2 - (\Delta k/2)^2]^{1/2}$, $\Delta k = k_p - k_s - k_i$ is the phase velocity mismatch, and $\Gamma^2 = (2|d_{\text{eff}}|^2 \omega_s \omega_i I_p)/(\varepsilon_0 n_s n_i n_p c^3)$, with ω the angular frequency, n the refractive index, and subscripts s, i, p denoting signal, idler, and pump [3]. Consequently a modest reduction in d_{eff} can result in a significant reduction in small-signal gain, which increases the threshold for oscillation and reduces the overall conversion efficiency. A higher oscillation threshold requires higher energy pump pulses, which increases the risk of optical damage, so the choice of non-optimum polarizations for the mixing waves is purely practical.

[1] The cavity Fresnel number is given by $\mathscr{F} = D^2/\lambda L$ where D is the beam diameter, λ the resonated wavelength – the signal at 1627 nm in this case – and L is the round-trip length of the cavity. $\mathscr{F}$ provides a measure of diffractive coupling across the transverse dimension of the beam with low $\mathscr{F}$ resulting in good beam quality and higher $\mathscr{F}$, say $\gtrsim 30$ for nanosecond OPO's, resulting in noticeably diminished beam quality. For example, a HeNe laser cavity that generates a lowest-order Hermite-Gaussian spatial profile has $\mathscr{F} \approx 1$.

[2] (o) denotes ordinary polarization, (e) denotes extraordinary polarization, and the arrow $\rightarrow$ indicates the desired direction of energy flow.

Although high optical conversion efficiency is important it is only one measure of the overall performance of an OPO, with beam quality often playing an equally important role. To improve beam quality the RISTRA cavity design uses image rotation in conjunction with birefringent walkoff to increase phasefront correlation[3] but its effectiveness at doing so depends on the size of the walkoff displacement – crystal length $\times$ walkoff angle – and on the polarizations of the mixing waves. Generally, large walkoff displacement due to larger birefringent walkoff angles, say $\gtrsim 50$ mrad, enhances the RISTRA's ability to improve beam quality, while small displacement from smaller walkoff angles, say $\lesssim 30$ mrad, reduces this ability. Ultimately the ratio of walkoff displacement to beam diameter, and of pump-pulse duration to cavity round-trip-time, together determine the degree of phase-front correlation and the ability of the RISTRA OPO to "clean up" a poor quality pump beam. The clean-up process is also susceptible to polarization, with its effectiveness enhanced when the pump- and resonated-waves have orthogonal polarizations, and reduced when they share the same polarization. Unfortunately the required choice of mixing at $\theta = 72.9^\circ$ in *xz*-cut KTP carries this "shared polarization" penalty, and is also accompanied by a walkoff angle of only 25.86 mrad, compared to 48.15 mrad for the other *xz*-cut at $\theta = 45.1^\circ$. This choice of non-optimum mixing doesn't eliminate beam clean-up, but it does result in greater susceptibility of the resonated wave to the spatial characteristics of the pump-beam. As a result, if the transverse spatial profile of the pump is asymmetric, or modulated by ring structure, or has wavefront aberration due to thermally induced distortion, the beam quality of the OPO's resonated wave will likely suffer. This can be particularly true for broadband oscillation in the non-planar RISTRA OPO, especially if the cavity Fresnel number is large, because the resulting admixture of its non-degenerate right- and left-helicity Laguerre-Gaussian modes, can lead to a structured signal beam with increased divergence.

[3]This is fancy language to say that image rotation, working in conjunction with birefringent walkoff, smooths-out and flattens lumpy, aberrated phase fronts, with the goal of obtaining flat phase across the entire beam diameter, that is, 100% phasefront correlation. Image rotation can also result in averaging and smoothing of the spatial fluence profile. Note that we might interchangeably use the term wavefront for phasefront.

2 Results and discussion

Section 1 provides a short but necessary background of RISTRA OPO operating principles. It was included here to help understand how pump-beam spatial properties, and the selection of nonlinear mixing parameters, can affect OPO performance. And unfortunately the Inlite laser, with its donut-like spatial profile, provides an interesting case study of these effects. The Inlite's spatial fluence profile is shown in the contour plot in Fig. 1 along with vertical and horizontal slices through the center of the beam. As described in Sec. 1 a pump beam with a semi-hollow center is a poor choice for pumping RISTRA OPO's.

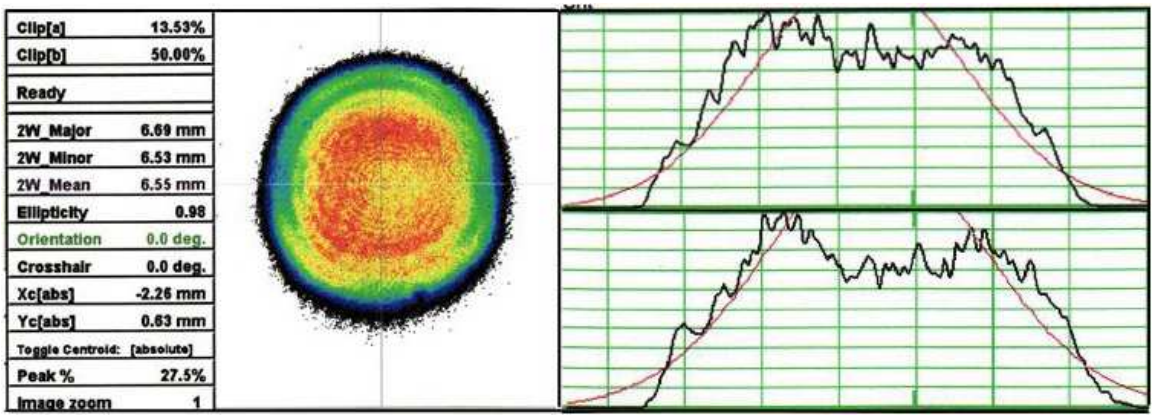

Figure 1. Spatial fluence contour plot and transverse slices for the Continuum Inlite laser beam (provided by Continuum).

Although the Inlite is not injection seeded, its spectral bandwidth is sufficiently narrow to allow non-quantitative wavefront characterization using a shearing-plate interferometer. These measurements revealed desirable characteristics of low divergence with little wavefront aberration, however when the Inlite's beam is coupled with a RISTRA cavity those good features are overwhelmed by the Inlite's donut-shaped profile, where the peak-to-valley fluence differs as much as 30%. Given the beam diameter is about 6.5 mm – near the approximately 7.5–8 mm limit for the RISTRA cavity – this profile has particularly deleterious effects for broadband oscillation because the higher fluence at its perimeter readily excites the RISTRA's non-degenerate off-axis modes.

Based on results from similar work carried out at Sandia Labs for a 1064 nm pumped potassium titanyl arsenate (KTA) RISTRA OPO [4], the KTP RISTRA's signal energy was lower than expected. The signal beam also contained substantial spatial structure and had higher than expected far field divergence of ~ 4 mrad. This is noteworthy because *xz*-cut KTA at $\theta = 67.2^\circ$ offers the same pump, signal, and idler polarizations as *xz*-cut KTP at $\theta = 72.9^\circ$ and the walkoff angle is only 4 mrad larger while d_{eff} is smaller at 2.89 pm/V. Nonetheless the KTA RISTRA achieved higher signal energy, and it also generated a higher quality signal beam. This was true even though one of the crystals contained refractive index inhomogeneities that induced beam distortion, a well known problem for KTA.

Although the pump laser for the KTA RISTRA was injection seeded to produce temporally transform limited pulses, a more important difference between it and the Inlite laser was its spatial fluence profile, which was smooth and peaked on axis, as shown below in Fig. 2. Using maximum pump energy of approximately 450 mJ the KTA RISTRA generated signal energy exceeding

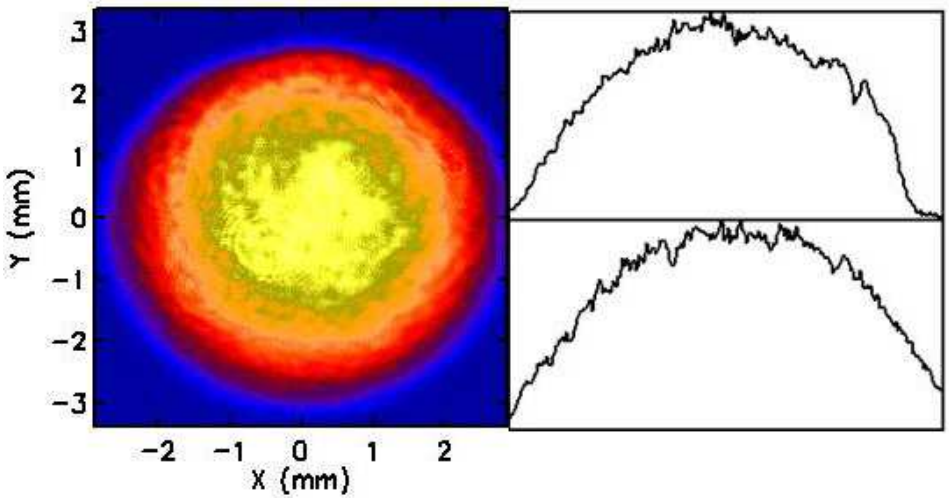

Figure 2. Spatial fluence contour plot and transverse slices for the pump beam used with the KTA RISTRA OPO. This pump beam spatial profile is peaked on axis and its diameter is 1–1.5 mm smaller than the pump beam from the Continuum Inlite. Data from Ref. [4].

150 mJ whereas the current KTP RISTRA achieved maximum energy of about 85–95 mJ for pump energy as high as 475 mJ. The use of two different signal wavelengths, 1550 nm and 1627 nm, and two different crystals, where d_{eff} is even smaller for KTA than for KTP, can't account for these substantial discrepancies. Another significant difference in the previous work was injection seeding of the KTA OPO at its signal wavelength. Seeding can reduce the oscillation threshold, increase conversion efficiency, and improve beam quality, but we note that maximum output energy varied by only a few percent for seeded and unseeded oscillation in the KTA OPO. Not surprisingly the KTA RISTRA's higher conversion efficiency was accompanied by much better signal beam quality, especially for seeded oscillation, however unseeded oscillation also produced better beam quality than we observed for the KTP RISTRA. We can only attribute these various conflicting observations to the difference in the spatial fluence profiles of the two pump lasers.

Because signal energy and beam quality were lower than anticipated for the KTP RISTRA, we considered several optional configurations that could improve performance. One is to replace the pump laser with another whose beam has spatial properties better suited to pumping OPO's. Unfortunately due to space and cost constraints that option is not available. Another is to decrease the pump beam diameter to reduce the cavity Fresnel number to improve the signal beam quality. A test of this approach was carried out by placing a Galilean telescope with $M = 0.5$ in the pump beam, and although the pump beam diameter was too small to achieve the minimum required signal

energy for the IACS platform of 50 mJ, the far field divergence decreased from about 4 mrad with the 6.5 mm pump beam to $\gtrsim 2$ mrad, as shown below in Fig. 3(b). As shown in Fig. 3(c) an addi-

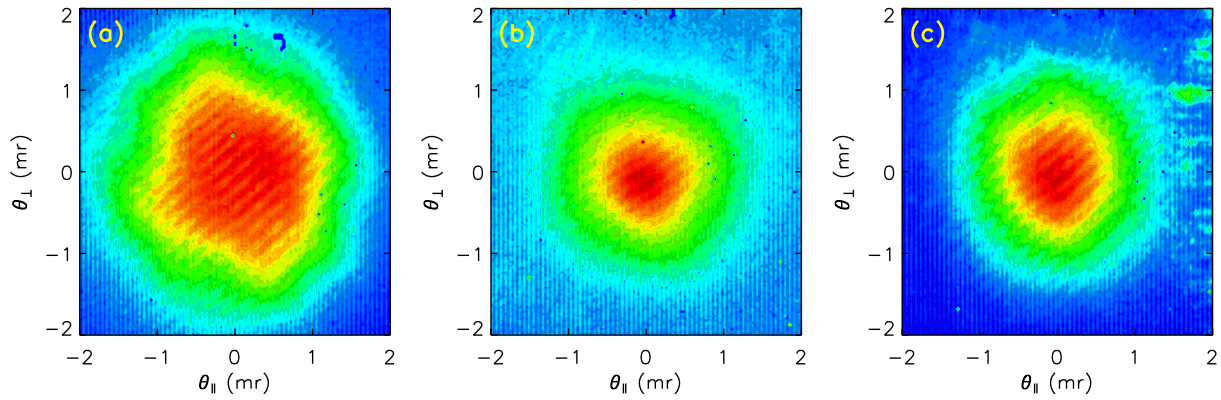

Figure 3. (a) Contour plot of far field OPO signal spatial fluence profile with pump beam diameter of ~ 6.5 mm, and (b) when the pump beam diameter was reduced using a Galilean telescope with $M = 0.5$, and (c) with $M = 0.5$ and Q-switch delay of $230\,\mu$sec. $\theta_\parallel$(mr) denotes the far field angle parallel to the direction of birefringent walkoff in milliradians, and $\theta_\perp$(mr) the far field angle in the perpendicular direction. Beam profiles were recorded using a Sensors Unlimited progressive scan InGaAs camera with pixel size of $30\,\mu$m and spatial resolution of 320×240. The vertical lines in the plots are residual readout noise which remains after background subtraction. The diagonal lines are interference fringes from the cover glass on the InGaAs array. Dark blue spots are pixels that are dead or permanently saturated. See text for additional details.

tional change in the spatial profile may be obtained by increasing the Inlite's Q-switch delay from its nominal setting of $190\,\mu$sec to $230\,\mu$sec to increase pump pulse duration by ~ 1 ns, however when this was done pump energy fell by an unacceptable $\geq 10\%$. All three signal spatial profiles shown in Fig. 3 were recorded with pump energy approximately 2.5–4$\times$ the oscillation threshold so that a semi-hollow center in the signal beam – a persistent characteristic of vortex beams – was mostly filled in. Near the oscillation threshold the influence of the off-axis vortex modes was more pronounced, especially in the near field. We note that for conventional nanosecond OPO cavities with $\mathscr{F} \gtrsim 200$ both of these far field divergence angles are considered moderate to small, however previous RISTRA OPO's with $\mathscr{F} \gtrsim 400$ yielded far field divergence angles ≤ 0.25 mrad [5]. An example of the far field fluence profile obtained from the injection seeded KTA RISTRA OPO with $\mathscr{F} \lesssim 200$ is shown in Fig. 4. The influence of the refractive index inhomogeneity in one of the crystals is evident by the sharp points in the low amplitude shoulder of the beam.

A final option for improving the Inlite's pump beam quality would involve pumping in the far field. This is not a commonly done but a measurement of the partially depleted 1064 nm pump

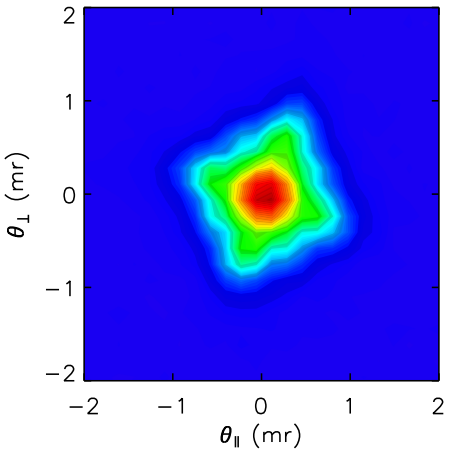

Figure 4. Contour plot of far field signal spatial fluence profile for the injection seeded KTA RISTRA OPO pumped by the beam shown in Fig. 2. $\theta_\parallel(\mathrm{mr})$ denotes the far field angle parallel to the direction of birefringent walkoff in milliradians, and $\theta_\perp(\mathrm{mr})$ the far field angle in the perpendicular direction. It's not uncommon for the far field fluence from a RISTRA OPO to have a low amplitude shoulder with four-fold symmetry but the sharpness of these features for the KTA RISTRA are enhanced by a refractive index inhomogeneity in one of its crystals. This profile from Ref. [4] was recorded by a Spiricon Pyrocam with 100 μm spatial resolution. It should be compared to the far field profile in Fig. 3(a). See text for additional details.

beam in the far field, shown in Fig. 5 revealed an asymmetric but otherwise Gaussian-like profile with low divergence, and we expect the undepleted profile to have similar, and perhaps better, beam quality. A Gaussian pump spatial profile is not optimum for achieving high conversion efficiency in nanosecond OPO's however it definitely has the potential improve beam quality. Nonetheless the propagation distance required for the pump spatial profile to freely evolve from donut to Gaussian-like could be many meters, and accessing the far field on the optical table using focusing followed by imaging with magnification, would likely be difficult to implement. Consequently this option is also impractical, however the far field measurement in Fig. 5 shows that the partially depleted pump beam can be used as a source of 1064 nm light as required for the IACS platform.

An alternative method to improve signal beam quality that may lessen dependence on the pump spatial profile is to injection seed the RISTRA OPO at the signal wavelength. Even though the Nd:YAG laser oscillates on multiple longitudinal modes, injection seeding the OPO would restrict the spectrum of its signal wave to essentially one on-axis mode and largely eliminate the off-axis vortex modes. This approach was successfully implemented by other workers using a two-crystal KTA RISTRA oscillating at 1550 nm that was pumped by another Continuum Inlite laser

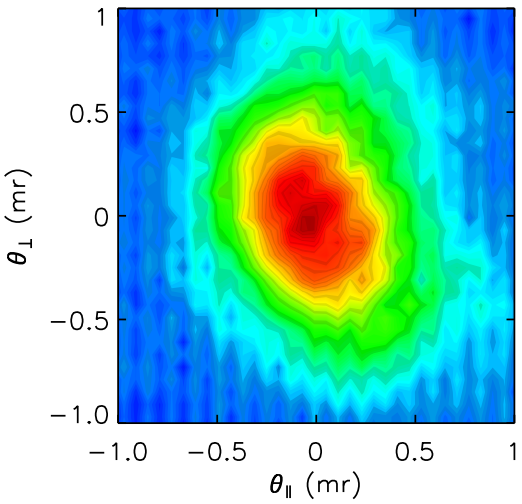

Figure 5. Contour plot of partially depleted pump beam in the far field. See text for additional details.

similar to the laser used by GTRI.[4] That laser also had a donut-shaped spatial profile and yet the resulting far field divergence was less than 0.5 mrad. Of particular interest in this second example of an Inlite pumped RISTRA was signal beam quality when the OPO was allowed to oscillate on multiple longitudinal modes. When oscillating without injection seeding, the far field divergence was similar to what we observe for the KTP RISTRA tested at GTRI. Unfortunately injection seeding GTRI's OPO is also not a practical or cost effective option for the IACS platform.

[4]Lockheed-Martin Coherent Technologies developed this system but the application cannot be disclosed

3 Observations and options for improved performance

As discussed in Secs. 1 and 2 the KTP RISTRA OPO performed below expectations but the causes of this diminished performance were identified and are well understood. To summarize the results of the risk reduction measurements we list our observations and describe options for improved performance.

- The donut-like spatial fluence profile of the Continuum Inlite pump laser was not a good choice for pumping the RISTRA OPO and it resulted in lower than expected output energy and reduced beam quality.
- The poor OPO signal beam quality can be attributed to an admixture of the RISTRA cavity's off-axis Laguerre-Gaussian modes that are readily excited by a donut-like pump beam.
- The OPO signal energy was approximately $2/3$ of what was previously achieved from a similar KTA RISTRA OPO developed and tested at Sandia National Labs that was pumped by a beam with a spatial profile that was peaked on axis and had a diameter of approximately 5.5 mm. The peaked beam excites the on-axis modes of the RISTRA which have higher gain, resulting in overall higher conversion efficiency.
- After examining various available options for improving the pump-beam quality, and by comparing various measurements carried out at GTRI, we conclude that the best compromise in terms of 1627 nm energy and beam quality will be obtained by placing the laser as close as possible to the OPO's input coupler. While this approach does not alter the pump-beam spatial fluence profile used in these measurements in any significant way, it results in the smallest pump beam diameter that can be obtained without resorting to the use of magnification.
- Although methods exist to improve beam quality and conversion efficiency such as injection seeding the OPO or replacing the pump laser altogether, they are not sufficiently cost effective nor practical for consideration at this time.

4 Predicted performance from numerical modeling

The numerical model used to predict performance of the KTP RISTRA OPO is a modified version of the 2D-cav-LP model from the standard SNLO distribution [6] that includes image rotation and permits two crystals in the RISTRA cavity having unequal lengths. This model simulates oscillation on a single longitudinal mode that closes after one round trip of the cavity. It could in principle be modified to simulate single-frequency oscillation on one of the off-axis vortex modes that close after four round trips, but a fully broadband model that would mimic operating conditions for GTRI's OPO – broadband pump pulse and broadband OPO, including all possible modes of oscillation – would be too numerically intensive for desktop computing and require migration to a super-computing platform. The effort required to achieve this capability would likely not be justified by the results. SNLO does contain a plane wave broadband model but it would be of limited value for simulating the operating conditions of GTRI's OPO.

Despite the inability to numerically simulate broadband operating conditions for the RISTRA OPO, the models are still of great value. They accurately compare relative conversion efficiency obtained from different crystals, such as KTP or KTA, and for different cuts of the same crystal. For example the models guided our selection of the *xz*-cut of KTP with $1064(o) \rightarrow 1627(o)+3074.8(e)$ over the alternative with $1064(o) \rightarrow 1627(e)+3074.8(o)$. The models also provide very good guidance for selecting output coupler reflectivity and for selecting crystal lengths.

The RISTRA model GUI with inputs for $1064(o) \rightarrow 1627(o)+3074.8(e)$ is shown in Fig. 6 along with efficiency curves – OPO signal energy plotted against pump energy – for three different operating conditions. For the *xz*-cut with $1064(o) \rightarrow 1627(o)+3074.8(e)$, referred to as (ooe) in Fig. 6, we show simulations with and without idler absorption, even though the absorption is very weak. We note that the ability to simulate effects such as idler absorption is powerful and in this case made clear there was no justification for the approximately $3\times$ higher cost of KTA, where idler absorption is slightly lower than in KTP. We also predicted the effect of lower d_{eff} for the *xz*-cut with $1064(o) \rightarrow 1627(e)+3074.8(o)$, labeled (oeo) in Fig. 6, and see a nearly $2\times$ increase in the oscillation threshold. While the experimental conditions for GTRI's KTP RISTRA OPO prohibit direct, fully quantitative comparisons to the model, we note that for single-frequency operation where all model input parameters are accurately measured, the SNLO models predict measured performance at the few percent level [7].

The RISTRA models can also predict beam quality but can only do so with high accuracy for single frequency oscillation. And although the two different cuts of KTP will show differences, with *oeo* producing higher quality beams, the accuracy of these predictions would obviously be diminished by broadband oscillation. With the difference in conversion efficiency due to smaller d_{eff} for the *oeo* cut we automatically choose *ooe*, independent of beam quality.

From the results in Fig. 6 it's clear that the broadband KTP RISTA OPO's conversion efficiency fell far short of model predictions. We note however that previous work at Sandia Labs with the 1064 nm pumped KTA RISTRA in Ref. [4] achieved better agreement with the models, although there were discrepancies for that work as well. In this work the large discrepancies between predicted and measured signal energy are not a surprise given the substantial admixture of off-axis

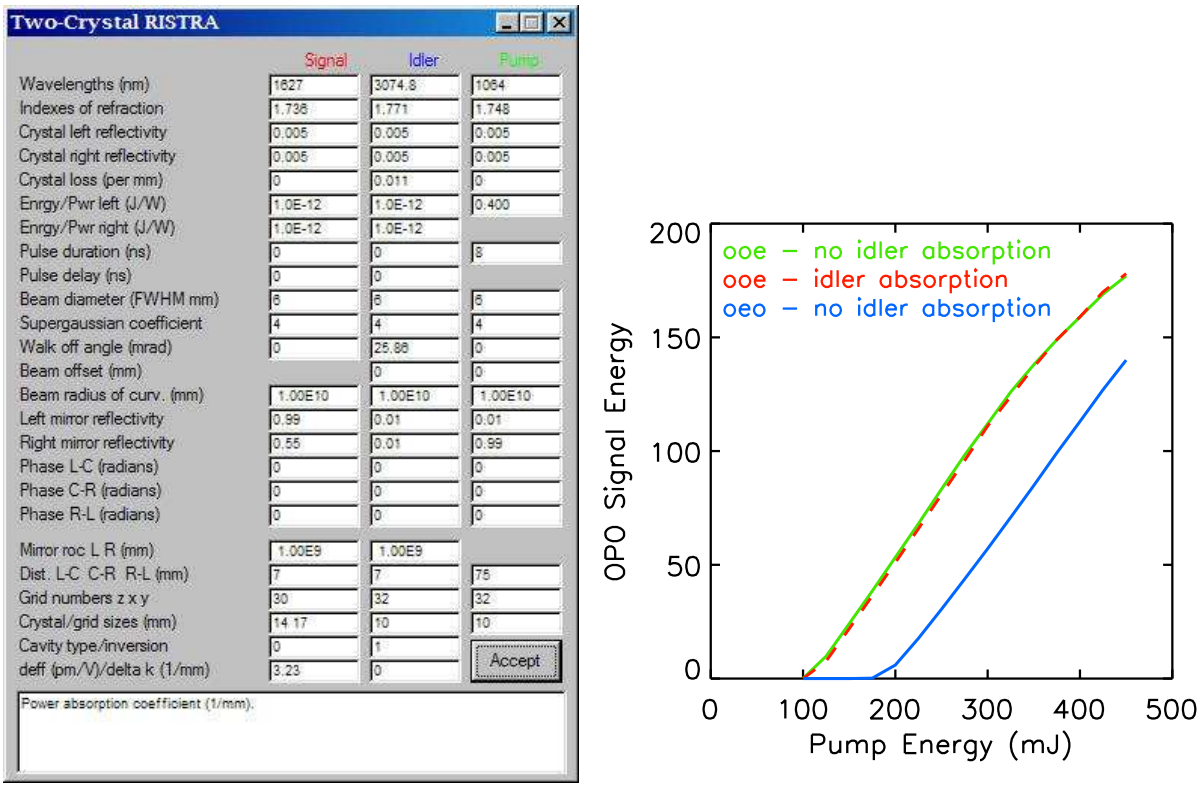

Figure 6. Model inputs for a RISTRA OPO using two unequal-length crystals for $1064(o) \rightarrow 1627(o) + 3074.8(e)$ at $\theta = 72.9°$ in *xz*-cut KTP. Efficiency curves for $1064(o) \rightarrow 1627(o) + 3074.8(e)$ (ooe) with and without idler absorption, and for $1064(o) \rightarrow 1627(e) + 3074.8(o)$ (oeo) without idler absorption.

modes. These modes provide much lower gain and and lower overall conversion efficiency.

Finally, as any seasoned experimenter knows all too well there's no substitute for testing performance in the lab. The discrepancies between predictions and measurements for the KTP RISTRA make clear that it would be unwise to omit risk reduction experiments form any development program.

A Components and suppliers

Although OPO beam quality and conversion efficiency were below expectations, the major components of the system otherwise performed well. We list here the major optical component suppliers, with comments:

- The OPO cavity mirrors were supplied Advanced Thin Films, Boulder, CO. Throughout these preliminary tests the mirrors suffered no damage and appear to meet or exceed all specifications. The mirrors use super-polished un-doped YAG substrates with ion beam sputtered (IBS) coatings.
- The double-wavelength intra-cavity half-wave retardation plates supplied by Meller Optics, Providence, RI, are fabricated from sapphire and appear to meet all specifications.
- The KTP crystals were supplied by ITI Electro Optics, Los Angeles, CA and were AR-coated by Thin Film Lab, Milford, PA, and the crystals and coatings also appear to meet all required specifications.

B RISTRA cavity name conventions and mirror specifications

CAVITY CONFIGURATION AND NAME CONVENTIONS

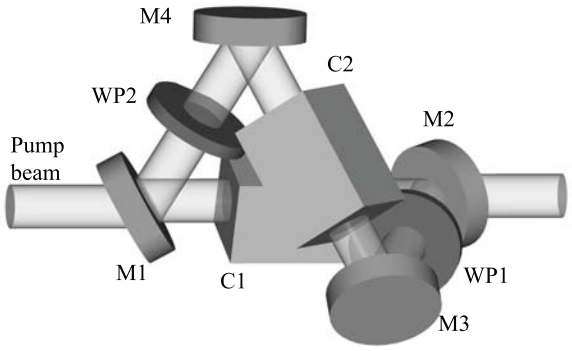

Two-crystal RISTRA cavity (denotes rotated-image singly-resonant twisted rectangle). M1–M4 = cavity mirrors; WP1 and WP2 = $\lambda/2$ retardation plates for 1064 nm and 1627 nm; C1 and C2 = nonlinear crystals.

NOTE: The pump beam enters through M1 and exits through M4. The propagation direction is M1→M2→M3→M4 with M2 the output coupler for the resonated signal wave at $\lambda = 1627$ nm.

CAVITY MIRROR SPECIFICATIONS

Nonlinear mixing: $1064(o) \rightarrow 1627(o) + 3074.8(e)$

θ = angle of incidence; R = reflectivity

Beam transmission through side 1 first, side 2 second

MIRROR 1: (Input coupler)

Side 1: $R \leq 0.25\%$, $\lambda = 1064$ nm, P-polarization, $\theta = 32.8^\circ$
$R \leq 0.25\%$, $\lambda = 1627$ nm, P-polarization, $\theta = 32.8^\circ$
$R \leq 4\%$, $\lambda = 3075$ nm, S-polarization, $\theta = 32.8^\circ$

Side 2: $R < 0.25\%$, $\lambda = 1064$ nm, P-polarization, $\theta = 32.8^\circ$ (best effort: $R < 0.5\%$ acceptable)
$R \geq 99\%$, $\lambda = 1627$ nm, P-polarization, $\theta = 32.8^\circ$
$R \leq 4\%$, $\lambda = 3075$ nm, S-polarization, $\theta = 32.8^\circ$

MIRROR 2: (Output coupler)

Side 1: $R \geq 99\%$, $\lambda = 1064$ nm, S-polarization, $\theta = 32.8^\circ$

$R = 55\% \pm 2\%$, $\lambda = 1627$ nm, *S*-polarization, $\theta = 32.8^\circ$
$R \leq 4\%$, $\lambda = 3075$ nm, *P*-polarization, $\theta = 32.8^\circ$

Side 2: $R \leq 0.25\%$, $\lambda = 1064$ nm, *S*-polarization, $\theta = 32.8^\circ$
$R < 0.25\%$, $\lambda = 1627$ nm, *S*-polarization, $\theta = 32.8^\circ$
$R \leq 4\%$, $\lambda = 3075$ nm, *P*-polarization, $\theta = 32.8^\circ$

MIRROR 3:

Side 1: $R \geq 99\%$, $\lambda = 1064$ nm, *S*-polarization, $\theta = 32.8^\circ$
$R \geq 99\%$, $\lambda = 1627$ nm, *S*-polarization, $\theta = 32.8^\circ$
$R \leq 4\%$, $\lambda = 3075$ nm, *P*-polarization, $\theta = 32.8^\circ$

Side 2: $R \leq 0.25\%$, $\lambda = 1064$ nm, *S*-polarization, $\theta = 32.8^\circ$ (S2 on M3 identical to S2 on M2)
$R < 0.25\%$, $\lambda = 1627$ nm, *S*-polarization, $\theta = 32.8^\circ$
$R < 4\%$, $\lambda = 3075$ nm, *P*-polarization, $\theta = 32.8^\circ$

MIRROR 4: (Pump exit: Identical to M1 with S1 and S2 reversed)

Side 1: $R \leq 0.25\%$, $\lambda = 1064$ nm, *P*-polarization, $\theta = 32.8^\circ$ (best effort: $R < 0.5\%$ acceptable)
$R \geq 99\%$, $\lambda = 1627$ nm, *P*-polarization, $\theta = 32.8^\circ$
$R \leq 4\%$, $\lambda = 3075$ nm, *S*-polarization, $\theta = 32.8^\circ$

Side 2: $R \leq 0.25\%$, $\lambda = 1064$ nm, *P*-polarization, $\theta = 32.8^\circ$
$R \leq 0.25\%$, $\lambda = 1627$ nm, *P*-polarization, $\theta = 32.8^\circ$
$R \leq 4\%$, $\lambda = 3075$ nm, *S*-polarization $\theta = 32.8^\circ$

References

[1] A. V. Smith and D. J. Armstrong, "Nanosecond optical parametric oscillator with 90° image rotation: Design and performance," J. Opt. Soc. Am. B **19**, 1801–1814 (2002).

[2] A. V. Smith and D. J. Armstrong, "Generation of vortex beams by an image-rotating optical parametric oscillator," Opt. Express **11**, 868–873 (2003).

[3] D. J. Armstrong, W. J. Alford, T. D. Raymond, and A. V. Smith, "Absolute Measurement of the effective nonlinearities of KTP and BBO crystals by optical parametric amplification," Appl. Opt. **35**, 2032–2040 (1996).

[4] D. J. Armstrong and A. V. Smith, "150-mJ 1550-nm KTA OPO with good beam quality and high efficiency," Proc. SPIE **5337**, 71–80 (2004).

[5] D. J. Armstrong and A. V. Smith, "90% pump depletion and good beam quality in a pulse-injection-seeded nanosecond optical parametric oscillator," Opt. Lett. **31**, 380–382 (2006).

[6] Numerical models for nonlinear mixing in crystals for timescales ranging from femtosecond to cw are available in the SNLO software package package, written and distributed by Arlee V. Smith at AS-Photonics. SNLO contains 17 different software tools that can be used for design and testing of OPA's, OPO's, and to calculate nonlinear crystal mixing parameters. SNLO can be downloaded free of charge from http://www.as-photonics.com/. Special codes for various versions of the image-rotating RISTRA OPO are available on request .

[7] A. V. Smith, W. J. Alford, T. D. Raymond, and M. S. Bowers, "Comparison of a numerical model with measured performance of a seeded, nanosecond KTP optical parametric oscillator," J. Opt. Soc. Am. B **12**, 2253–2267 (1995).

Distribution:

1	MS 0899	Technical Library, 9536
2	MS 1423	G. A. Hebner, 1128

Sandia National Laboratories